INTERNATIONAL JOURNAL OF HYDROGEN ENERGY 47 (2022) 4814–4826

Available online at www.sciencedirect.com

ScienceDirect

journal homepage: www.elsevier.com/locate/he

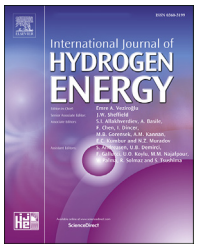

Parameter characterization of HTPEMFC using numerical simulation and genetic algorithms

Raúl Losantos [a], *Manuel Montiel* [a,b], *Radu Mustata* [a], *Fernando Zorrilla* [a], *Luis Valiño* [a,*]

[a] *LIFTEC, CSIC-Universidad de Zaragoza, C/María de Luna 10, Zaragoza, Spain*
[b] *Fundación ARAID, Gobierno de Aragón, Spain*

HIGHLIGHTS

- Transfer coe_cients and exchange currents estimation in HTPEMFCs using simulations.
- Estimation of the radius of agglomerates and the thickness of the ionomer in HTPEMFCs.
- Characterization of a HTPEMFC using 3D numerical simulations with genetic algorithms.
- Using measurements, electrochemical parameters are found that fit a 3D model.

ARTICLE INFO

Article history:
Received 25 June 2021
Received in revised form
11 September 2021
Accepted 11 November 2021
Available online 15 December 2021

Keywords:
PEMFC
HTPEMFC
Model parameter estimation
Genetic algorithm

ABSTRACT

This paper develops a novel approach to the parameterisation of high temperature exchange membrane fuel cells (HTPEMFC) with limited and non-invasive measurements. The proposed method allows an effective identification of electrochemical parameters for three-dimensional fuel cell models by combining computational simulation tools and genetic algorithms. To avoid each evaluation undertaken by the optimisation method involving a complete computational simulation of the 3D model, a strategy has been designed that, thanks to an iterative process, makes it possible to decouple the fluid dynamic resolution from the electrochemistry one.

Two electrochemical models have been incorporated into these tools to describe the behaviour of the catalyst layer, Butler-Volmer and spherical aggregate. For each one, a case study has been carried out to validate the results by comparing them with empirical data in the first model and with data generated by numerical simulation in the second. Results show that, from a set of measured operating conditions, it is possible to identify a unique set of electrochemical parameters that fits the 3D model to the target polarisation curve. The extension of this framework can be used to systematically estimate any model parameter in order to reduce the uncertainty in 3D simulation predictions.

* *Corresponding author.*
E-mail address: l.valino@csic.es (L. Valiño).

https://doi.org/10.1016/j.ijhydene.2021.11.084

List of symbols

a	Effective surface area (m^{-1})
C	Mass fraction
D	Diffusivity ($m^2\ s^{-1}$)
E	Energy activation ($J\ mol^{-1}$)
E_r	Efficiency factor of agglomerates
f	Platinum mass ratio to Pt/C
F	Faraday constant ($C\ mol^{-1}$)
H	Henry constant ($Pa\ m^3\ mol^{-1}$)
I	Cell current (A)
j	Exchange current density ($A\ m^{-2}$) or ($A\ m^{-3}$)
k	Reaction rate (s^{-1})
K	Permeability (m^2)
L	Volume fraction
M	Molecular weight ($kg\ mol^{-1}$)
m	Mass loading ($kg\ m^2$)
n	Number of transfer electrons
N	Theoretical reversible cell potential (V)
P	Pressure (Pa)
R	Universal gas constant ($J\ mol^{-1}\ K^{-1}$)
s	Number of locations
r	Agglomerate radius (m)
t	Thickness (m)
T	Temperature (K)
$\vec{u}$	Velocity vector ($m\ s^{-1}$)
V	Cell voltage (V)
x	Mole fraction
z	Number of polarisation points

Greek Letters

α	Transfer coefficient
γ	pressure dependency coefficient
δ	Thin film thickness (m)
ε	Porosity
η	Over-potential (V)
ρ	density ($kg\ m^{-3}$)
μ	Dynamic viscosity ($Pa\ s$)
σ	Proton conductivity ($S\ m^{-1}$)
Φ	Thiele Module
φ	Potential (V)

Superscripts and Subscripts

a	Anode
agg	Agglomerate
c	Cathode/carbon
cl	catalyst layer
cla	Anode catalyst layer
clc	Cathode catalyst layer
eff	Effective
exp	Experimental
i	Reactants, H_2, O_2 or H_2O/Ionomer
ref	Reference conditions
p	Protonic
PA	Phosphoric acid
Pt	Platinum
sim	Simulation

Introduction

Fossil fuel depletion and environmental issues have brought attention to the need for a change in the current energy model. The aim is to find new solutions for generating energy in a clean way that also guarantees the safety of supply and the current consumption model. In this context, increasingly affordable renewable energies seem to be the optimal choice and consequently their use has experienced exponential growth in recent years [1]. However, their intermittent generation requires the availability of storage systems, named energy vectors, which allow energy use to be deferred and at the same time facilitate its transport. Among them, hydrogen is a promising candidate, since it is obtained by electrolysis of water, a very abundant resource in nature, and does not generate pollution at the point of use. In addition, its storage and transportation could potentially utilise facilities already available to current vectors such as natural gas [2]. In contrast, it has a low volumetric energy density, which makes both its storage and transport more troublesome.

To recover the chemical energy contained in hydrogen, the most efficient process is the electrochemical combination with oxygen from the air, to form water and electrical energy. This conversion is carried out by the fuel cells. In particular, high temperature Proton Electrolyte Membrane fuel cells (HTPEMFC) are promising devices for power distribution systems, firm candidates for their applications in both transport and stationary use. However, their technological development continues to have important shortcomings and requires significant advances in order to be commercially competitive.

Numerical modelling and computer simulation make it easier and more affordable to understand the processes that take place inside the fuel cells, as well as serving as a tool to refine their designs. It has special relevance in the analysis of catalyst layers, as their thickness and manufacturing process make it difficult to observe the electrodynamic and physical phenomena taking place experimentally. As an example of numerical simulation analysis capabilities, Ebrahimi et al. [3] proposed a method to optimise the distribution of platinum particles along the catalyst layers.

Modelling of a fuel cell must describe the transport phenomena of gases and species through its channels and porous areas, the electrochemical reactions taking place in its catalyst layers and the transport of protons through its membrane. It is necessary to find a trade-off between the level of complexity of the model and the computational effort required to numerically solve it.

According to the literature, there are two types of approaches in these models [4], which are usually complementary. The first one includes mechanistic models, which aim to simulate the heat, mass transfer, and some electrochemical phenomena. The second one is used with models based on empirical or semi-empirical equations, which may also have a background in mechanistic models. This latter approach is used to explain the electrochemical phenomena, which are more complex to accommodate in mechanistic models. This involves tuning parameters so that the model fits the measurements obtained for each device. Effective parameter characterisation is a necessary step to release the full

predictive power of physics-based models, since the reliability of the models depends to a large extent on these parameter values.

During the last few years, the parameter estimation of the electrochemical model has attracted a considerable amount of attention. More specifically, it has been claimed to provide an industrially relevant example of a complex, nonlinear optimisation task. In particular, heuristic and meta-heuristic search methods have been applied to the parameter estimation problem.

Due to limitations in terms of computational cost, most approaches use zero-dimensional, semi-empirical equivalent circuit models, which are simplified, lumped representations of the physical and electrochemical mechanisms involved in fuel cells. Avoiding the spatial resolution of the problem allows us to reduce the resolution time of the model, which makes them particularly useful for studying the behaviour and interactions of fuel cells in energy systems.

Therefore, research has focused on the implementation of optimisation algorithms that improve search effectiveness and reduce parameter identification times. Several numbers of methods have been proposed in recent years for parameter model identification of the PEMFC, for example, Gray Wolf Optimizer by Ali et al. [5], Genetic Algorithm by Ariza et al. [6], Cuckoo Search Algorithm by Zhu et al. [7], Deer Hunting Optimisation Algorithm (DHOA) by Brammya et al. [8], Coyote Optimisation Algorithm by Yuan et al. [9], Monarch Butterfly Optimisation Algorithm by Bao et al. [10], Artificial ecosystem optimizer by Rizk et al. [11] and Levenberg-Marquardt backpropagation algorithm by Yang et al. [12].

A comparison between 45 references of parameter identification methods in zero-dimensional models is reported in Ohenoja et al. [13]. The report analyses some relevant aspects of these processes such as the optimisation method used, the number of parameters to be identified, their search ranges or the number of data points used in the optimisation.

Nevertheless, the parameters identified by this approach cannot be used in the computational simulation of dimensional models. While they are useful in the control and prediction of integrated systems, they do not allow a complete analysis of the inner workings of the fuel cell.

The fact that parameter identification remains a lesser studied topic in the fuel cell dimensional models can be mainly attributed to the computational cost of the available physics-based models that do not lend themselves to the systematic parameterisation of optimisation-based models, which typically require a large number of model evaluations. However, some researchers in the fuel cell community have developed studies in this field. Dobson et al. [14], combine 2D simulations model with computational optimisation, although this type of strategy is still burdened by the need to simplify the meshes used. A more recent work, developed by Goshtasbi et al. [15], uses characterisation techniques to identify a large number of parameters and thus rely less on the parameters of the literature. A pseudo-2D numerical model is used to reduce calculation times.

In both cases, these are simplified models of the device that do not allow a complete analysis of the spatial phenomena, especially in the case of devices with complex geometries.

The novelty introduced by this article is the development of a parameter identification strategy that integrates full 3D computational simulation models of HTPEMFC and optimisation through genetic algorithms. The obtained parameters can then be used directly in 3D simulations with predictive capabilities.

The remaining part of the article is structured as follows: in Section HTPEMFC Model and relevant parameters, the mathematical model of the fuel cell is explained briefly. Section Characterisation process description presents the optimisation algorithm and the process of parameter characterisation. Section Results and discussions provides the results of the characterisation applied to two cases and the work is concluded in Section Conclusions.

HTPEMFC model and relevant parameters

The proposed model is a 3D steady state, isothermal, incompressible flow model with further assumptions:

- Infinitely thin catalyst layers.
- High temperature fuel cell (single-phase gas flow).
- Migration of H^+ protons through the membrane obeying Onsager's principle, Valiño et al. [16]. Therefore there is a one-to-one match between the current densities at the anode and at the cathode catalyst layers, that is, $j_a = j_c$.
- The electrical potential is constant along the electrodes.

$$\nabla\cdot(\rho\vec{u}) = 0 \tag{1}$$

$$\nabla\cdot(\vec{u}C) = \nabla\left(D^{eff}\nabla C\right) \tag{2}$$

$$\frac{1}{\epsilon^2}\nabla\cdot(\rho\vec{u}\vec{u}) = -\nabla P + \frac{1}{\varepsilon}\nabla(\mu\nabla\vec{u}) - \frac{\mu\vec{u}}{K} \tag{3}$$

$$\varphi^p_{clc} - \varphi^p_{cla} = \frac{j}{\sigma} = N - \eta_c - \eta_a - V \tag{4}$$

The equations governing the operation of the fuel cell under the previous assumptions, include those of conservation of mass and momentum (Navier Stokes), species transport, electrochemical phenomena in the catalyst layers and transport of protons across the membrane. Fig. 1 shows schematically the domains where each equation is solved with its corresponding boundary conditions.

The theoretical reversible cell potential, N, at given pressure and temperature conditions is calculated by the Nernst equation.

$$N = N_{ref} + \frac{RT}{nF}\cdot\ln\left(\frac{P_{H_2}\cdot P^{0.5}_{O_2}}{P_{H_2O}}\right)(V) \tag{5}$$

Two electrochemical models have been incorporated in order to describe the relationship between current density and overpotential in the catalyst layers:

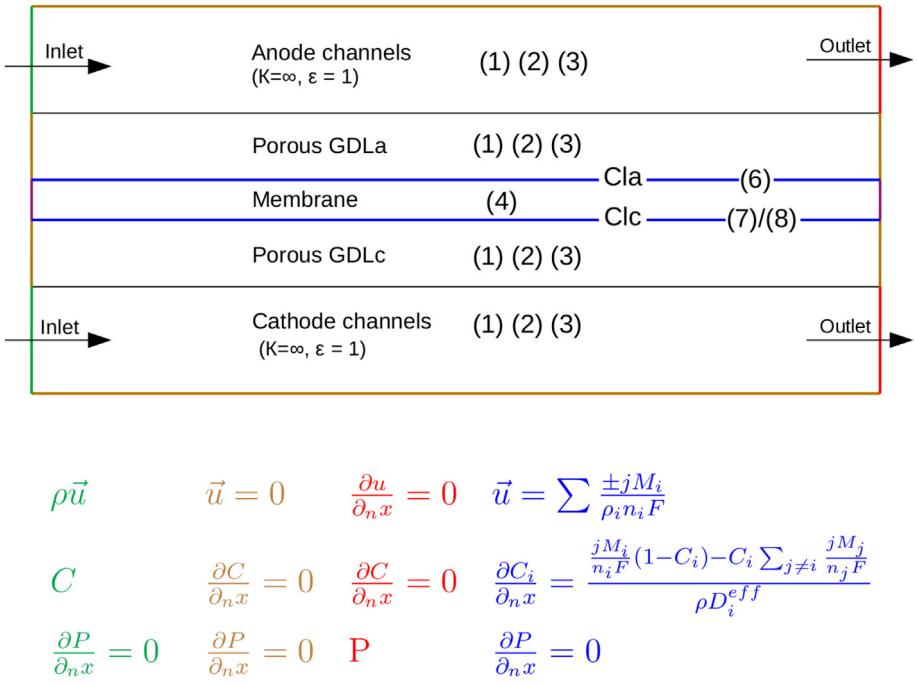

Fig. 1 – Outline of equations, boundary conditions and domains where they apply. Colours indicate the locations where each boundary condition is applied. Sub-indices i and j refer to the reactive species involved in each region, H_2 at the anode and O_2 and H_2O at the cathode.

Table 1 – Formulas for the agglomerate model of the catalyst layer. The reaction rate equation has been adapted by considering $\alpha_{Rd} = -\alpha_c$ and $\alpha_{Ox} = -(1-\alpha_c)$.

Parameter	Expression	Source
Effective agglomerate area (m^{-1})	$a_{agg} = \frac{3L_{Pt/C}\varepsilon_{CL}}{r_{agg}^3(1-L_{i,agg})}(r_{agg}+\delta_i)^2$	[19]
Volume fraction of platinum particles	$L_{Pt/C} = \frac{m_{pt}}{t_{CL}}\left(\frac{1}{\rho_{pt}}+\frac{1-f}{f}\frac{1}{\rho_c}\right)$	[19]
Volume fraction of the void space	$\varepsilon_{cl} = 1 - L_{Pt/C} - L_i$	[19]
Thickness of the ionomer film (m)	$\delta_i = r_{agg}\left[\sqrt[3]{\frac{L_i(1-L_{i,agg})}{L_{Pt/C}}} - L_{i,agg} + 1 - 1\right]$	[19]
Efficiency factor of agglomerates	$E_r = \frac{1}{\Phi}\left(\frac{1}{\tanh 3\Phi}-\frac{1}{3\Phi}\right)$	[19]
Thiele Module	$\Phi = \frac{r_{agg}}{3}\sqrt{\frac{k_c}{L_{i,agg}^{1.5}D_{O_2}}}$	[19]
Reaction rate (s^{-1})	$k_c = \frac{j_{c,0}^{ref}}{nF(1-\varepsilon_{cl})C_{O_2}^{ref}}\left(e^{\frac{\alpha_c F\eta_c}{RT}} - e^{\frac{-(1-\alpha_c)F\eta_c}{RT}}\right)$	[20]
O_2 diffusivity in ionomer (m^2s^{-1})	$D_{(i)O_2} = \frac{(42.4C_{PA}^3 - 110.1C_{PA}^2 + 95.3C_{PA} - 27.4)\times 10^{-3}}{e^{\frac{89449C_{PA}^2 - 155346C_{PA} + 71429}{T}}}$	[21]
Henry constant ($Pa\ m^3mol^{-1}$)	$H_{o_2} = e^{\left(\frac{(-1.27C_{PA}+1.23)\times 10^4}{T} + 35.2C_{PA} - 46.6\right)}$	[20]
PA mass fraction	$C_{PA} = \frac{0.0544x_{PA}}{(x_{PA}(0.0544-0.01)+0.01)}$	[20]
PA mole fraction	$x_{PA} = \frac{\ln(P_{H_2O}) + \frac{2765.1}{T} - 22.002}{\frac{-4121.9}{T} + 2.5929}$	[20]

Table 2 – Physical properties and operation conditions.

Parameter		Value
Membrane thickness (m)	L	2×10^{-4}
Inlet stoichiometric ratio		4
Inlet mass concentration	C_{H_2O}	0.5
(anode)	C_{H_2}	0.5
Inlet mass concentration	C_{H_2O}	0.5
(cathode)	C_{O_2}	0.5
Temperature (K)	T	393
Universal gas constant ($J\ mol^{-1}\ K^{-1}$)	R	8.31472
Faraday constant ($C\ mol^{-1}$)	F	96487
Reference pressure (atm)	P^{ref}	1
Reference temperature (K)	T^{ref}	298.15
Energy activation Anode ($J\ mol^{-1}$)	Ea	25000
Energy activation Cathode ($J\ mol^{-1}$)	Ec	66000
Protonic conductivity ($S\ m^{-1}$)	σ	1.2
Porosity	ε	0.5
Anode pressure dependency coefficient	γ_a	0.5
Cathode pressure dependency coefficient	γ_c	1

Butler-Volmer

In this model, the surface current density is related to the overpotential in the catalyst layers according to the expressions 6 and 7. This relationship is determined by the operating conditions, such as the partial pressure of the reactants P_{O_2}, P_{H_2}, the temperature in the catalyst layers, T, and also by other parameters, most of which are known a priori, and are listed in Table 2.

$$j_a = j_{a,0}^{ref} \cdot \left(\frac{P_{H_2}}{P^{ref}}\right)^{\gamma_a} e^{\left[\frac{-E_a}{R}\left(\frac{1}{T}-\frac{1}{T^{ref}}\right)\right]}\left(-e^{\frac{-\alpha_a F \eta_a}{RT}}+e^{\frac{(1-\alpha_a)F\eta_a}{RT}}\right)(A\,m^{-2}) \quad (6)$$

$$j_c = j_{c,0}^{ref} \cdot \left(\frac{P_{O_2}}{P^{ref}}\right)^{\gamma_c} e^{\left[\frac{-E_c}{R}\left(\frac{1}{T}-\frac{1}{T^{ref}}\right)\right]}\left(e^{\frac{\alpha_c F \eta_c}{RT}}-e^{\frac{-(1-\alpha_c)F\eta_c}{RT}}\right)(A\,m^{-2}) \quad (7)$$

However, some of the electrochemical properties are not easy to measure. Such is the case for the anodic and cathodic charge transfer coefficients, α_a and α_c, which physically represent the fraction of additional energy entering the oxidation and reduction reactions [17]. Their values depend on the type and conditions under which the reaction takes place and on the material of the electrodes. In practice they are fitting parameters.

In the above model $j_{a,0}^{ref}$ and $j_{c,0}^{ref}$ are defined as the exchange current density per unit of geometric area at reference pressure and temperature. Its value depends on the amount of platinum and the resulting geometry of the catalyst layers; hence it is generally difficult to be evaluated precisely a priori. These four variables are chosen to be the object of this characterisation process for the Butler-Volmer model.

Agglomerate

This model arises as a method for taking into account the microstructure of the catalyst layer, which is composed of platinum and carbon particles bonded together by the ionomer to form agglomerates. It has the ability to capture the loss of oxygen concentration at the platinum interface at high current densities. The reaction kinetics of the cathode catalyst layer is well known to be the limiting factor of the reaction in fuel cells and therefore it is only in the cathode where the model is implemented. This is due to the fact that the cathode reaction rate is several orders of magnitude lower than the anode one [18].

The spherical agglomerate model described by Dobson et al. [14] has been taken as a reference. This model is derived from the Butler-Volmer equation and incorporates a group of expressions that allow the characteristics of the agglomerates to be related to the phenomenon of losses due to concentration. According to the above-mentioned model, the catalyst layer is treated as a volume and therefore the current appears as a source term. To accommodate these expressions to the assumption of a layer of negligible thickness, appropriate modifications have been made so that the expression refers to the surface current density. Taking these considerations into account, the current density in the cathode catalyst layer is described by Equation (8), with terms as listed in Table 1.

$$j_c = t_{CL} n F P_{O_2} H_{O_2}\left(\frac{1}{E_r k_c (1-\varepsilon_{cl})}+\frac{(r_{agg}+\delta_i)\delta_i}{a_{agg} D_{O_2}}\right)^{-1}(A m^{-2}) \quad (8)$$

The set of expressions contained in Table 1 describes the relationship between current density and overpotential in the cathode according to the operating conditions, i.e. partial pressure of oxygen, P_{O_2}, the temperature in the catalyst layer, and a list of parameters that define the properties of the reaction. A sketch of the internal structure of the catalyst layer is shown in Fig. 2 in order to visualise the physical meaning of the parameters included in the equations of this model.

The volume fraction of platinum particles $L_{Pt/C}$, and the volume fraction of ionomer in the catalyst layer L_i, are known as they depend on the amount of material added during manufacture and the resulting thickness of the catalyst layer. However, in order to fully define the geometry of the agglomerates, it is necessary to know other parameters which, due to their nature, are extremely difficult to measure without invasive methods. These are the radius of the agglomerates, r_{agg}, and the thickness of the ionomer film over the agglomerate δ_i. Both depend on not only how the platinum particles are clustered and how the ionomer is distributed during the manufacturing process of the catalyst layers, but also on the degradation processes that occur during the operation of the fuel cell. Therefore, in the selection of the parameters to be characterised, δ_i and r_{agg} have been chosen, in addition to those already highlighted for the Butler-Volmer model (α_a, α_c, $j_{a,0}^{ref}$ and $j_{c,0}^{ref}$).

Characterisation process description

The aim of the optimisation is to find a combination of the electrochemical parameters mentioned in Section HTPEMFC Model and relevant parameters, which allows us to fit the points of the simulated polarisation curve into those available experimentally. For this purpose, genetic algorithms, which are computational evolutionary techniques for optimisation problems based on the selection of the fittest individuals, will be used. Fig. 3 shows a schematic of the evolutionary process.

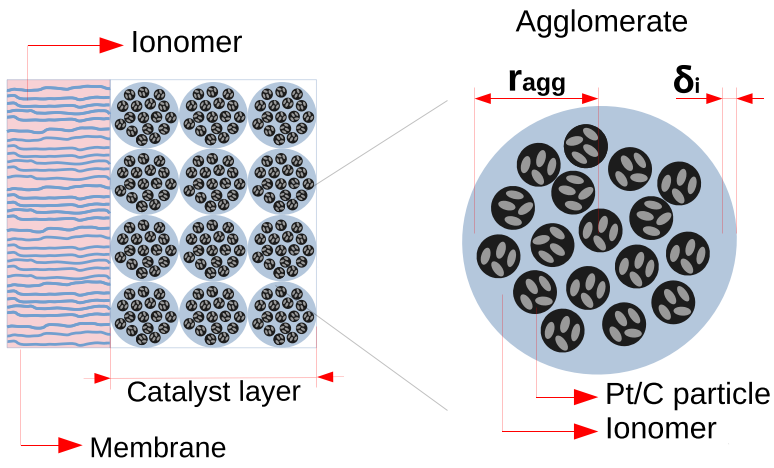

Fig. 2 – Schematic of the catalyst layer agglomerate structure.

According to the implemented system, each individual in the population corresponds to a potential solution, that is a combination of values of the parameters to be optimised. For example, for the Butler-Volmer model, one individual would be one set of possible values of $\left\{\alpha_a, \alpha_c, j_{a,0}^{ref}, j_{c,0}^{ref}\right\}$. The goal is to choose the best individual, that is, the four-dimensional set which is the best approximation of the experimental voltages.

The problem with implementing this type of evolutionary process with 3D models is that the computational cost of performing a numerical simulation for each individual evaluated would result in an unaffordable use of computing resources and time. To overcome this limitation, an iterative process is implemented which uncouples the fluid dynamics resolution from the electrochemical one during the evaluation of each individual by the genetic algorithm. This strategy makes sense because all the parameters needing characterisation are electrochemical. During the evaluation of each individual, the flow field is frozen, so only non-fluid related equations need to be solved, which are numerically much simpler. Once the best individual is found, the fluid dynamics is updated by a full 3D simulation (in fact, one per measured point in the polarisation curve to compare) and with the updated fluid fields, a new genetic algorithm search is launched. The process is repeated until simulated and experimental voltages converge. This procedure is explained in more detail below.

Experimental data

Experimental operating data of the analysed fuel cell should be available in order to proceed with the characterisation process. The points of the polarisation curve must be provided for stationary operating conditions. Besides the voltage and current values, it is necessary to know the conditions in which they have been obtained. That is to say, the flow and concentrations of the supplied species and the operating temperature at each point of the polarisation curve to be considered for fitting. It is important that the data collection is carried out in optimal conditions and with the appropriate measuring equipment, since the correct characterisation of the parameters depends largely on the reliability of the data obtained. In addition, it is required to gather the characteristics of the fuel cell used and its properties to be introduced in the computer simulation models. This includes, the geometric data of the fuel cell, the known electrochemical properties of the catalyst layers or the proton conductivity of the membrane.

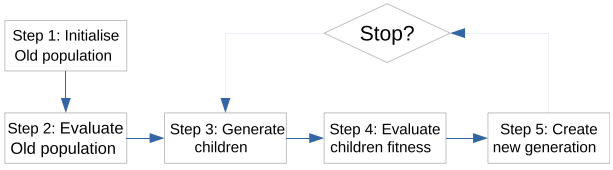

Fig. 3 – Evolutionary loop of populations in the genetic algorithm.

General iteration

The procedure for advancing one general iteration step is described next, leaving the particularities of the initial iteration for the next subsection. We start from the optimal individual selected by the genetic algorithm in the previous iteration. It must be reminded that the optimal individual provides the best fit for the measured voltages given in the polarisation curve. With the parameters of the optimal individual and the information provided by the experimental measurements (boundary conditions, chosen intensity and necessary physical coefficients) the equations of the fuel cell in section HTPEMFC Model and relevant parameters can be solved. Using the solution of the previous iteration as the initial condition, convergence is fast. Solutions are to be obtained for each measurement point of the polarisation curve. From this moment on during the present iteration, the fluid dynamics field solutions are considered frozen.

Next, the genetic algorithm needs to evaluate individuals, that is, sets of the electrochemical parameters (the ones needing characterisation) by calculating their associated voltages. Diagram 9 shows the relationships (via equations in section HTPEMFC Model and relevant parameters including boundary conditions) between the physical magnitudes

involved in the numerical calculation of the voltage. Once the fluid dynamics is frozen, so are the partial pressures at the catalyst layer and the surface current densities at the catalyst layers j_a, j_c. Both sets of quantities are directly linked by the fluid dynamics Equations (1)–(3) and boundary conditions). With those quantities fixed, the voltage V would only depend on the electrochemical parameters, according to the electrochemical Equations (4)–(6), 7/8). Hence, the genetic algorithm only needs to solve the electrochemical equations for evaluating individuals, which is computationally very fast.

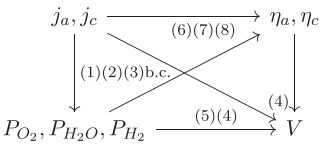

(9)

For each individual, one voltage distribution is obtained per measured point of the polarisation curve. Notice that the predicted voltage should be constant along the electrodes, but this is not guaranteed during this phase of the iterative process due to the frozen distribution of j imposed. The best individual is chosen to be the one that minimises the distance between its predicted voltages and the constant ones measured experimentally:

$$min \sum_{i=1}^{z} \sum_{j=1}^{s} \left(V_{exp[i]} - V_{[i,j]}\right)^2, \tag{10}$$

where z describes the number of points of the polarisation curve collected in the experimental phase and s the number of locations selected per measured point in order to proceed with a discretised evaluation of the distance. $V_{exp[i]}$ is the experimental value of the fuel cell voltage for each point of the polarisation curve. $V_{[i,j]}$ includes all the voltage values obtained for a single set of parameters to be optimised. Notice that, due to the algebraic nature of the electrochemical equations, explicit calculations are only needed for the small set s of selected locations.

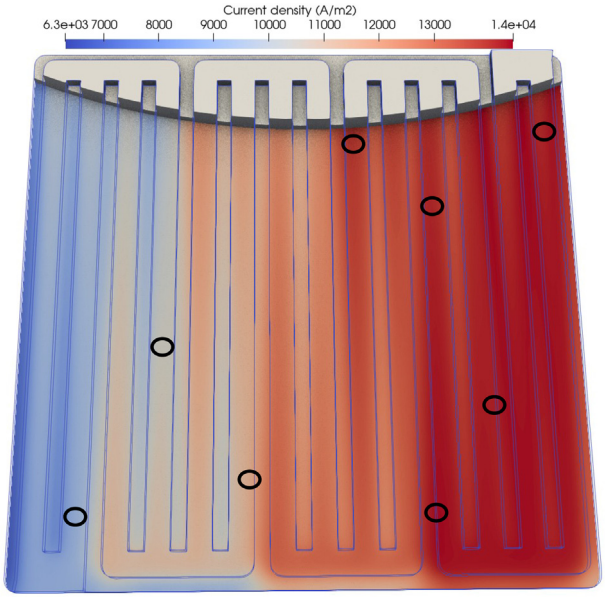

Fig. 4 – Current density distribution in the catalyst layer and the $s = 8$ selected locations for voltage calculation of the genetic algorithm.

Fig. 4 illustrates an example of the distribution of eight locations ($s = 8$) along the catalyst layer for the voltage evaluation of one individual. In order to select the representative locations, the software groups the information from the catalyst layers according to its oxygen partial pressure value P_{O_2}. The range of values of P_{O_2} obtained at the cathode catalyst layer is divided into s intervals, then for each interval, the location with the best local convergence is selected. Due to the iterative process of the 3D simulation process, there are local convergences of the electrochemical equations. This implies that, despite having a common convergence criterion, there are regions with a better correspondence and therefore these should provide information of a higher quality. Other reasonable criteria have been tested (consider intervals for j_c, locations homogeneously distributed), with a slightly lesser performance. These good behaviours are not surprising given the relative smooth distribution of physical magnitudes along the catalyst layers.

Fig. 5a and b illustrate graphically the adequacy between the calculated voltages and the experimental ones (see Equation (10)) for $z = 9$ and $s = 8$ for two individuals during the last iteration of a typical case, which actually corresponds to the second case presented in the next section. Fig. 5a shows the relatively poor behaviour of an individual of the first generations of the genetic algorithm. Genetic algorithms approach the solution by creating a new generation from the previous individuals, so younger generations are closer to the solution. Fig. 5b corresponds to the excellent agreement of the optimal individual (last generation). Each horizontal line represents the range of current densities values along the catalyst layer (see horizontal bar at the top of Fig. 4) corresponding to one measured point, which has the same experimental voltage.

The greater the number of location points, the better the quality of the estimation of the distance between the experimental and the calculated voltage for one individual. A higher s then implies that the genetic algorithm has a better estimation tool to obtain a solution closer to the one that satisfies all the operating conditions. However, this also means increasing the computational time. The selection of the optimal number of selected locations is therefore a trade-off between computational cost and required accuracy. This selection must also take into account the operating conditions of the fuel cell, since the greater the differences in the values along the catalyst layers, the greater the number of locations that allow smoothing the optimisation errors arising from the non-linearity of the electrochemical equations. In practice, as commented above, this is not an issue, given the relatively smooth distribution of physical magnitudes along the catalyst layers.

Notice also that the quality of the information provided to the genetic algorithm, and therefore the results it provides, depends on the agreement of the simulated conditions of partial pressures of reactive species and current densities

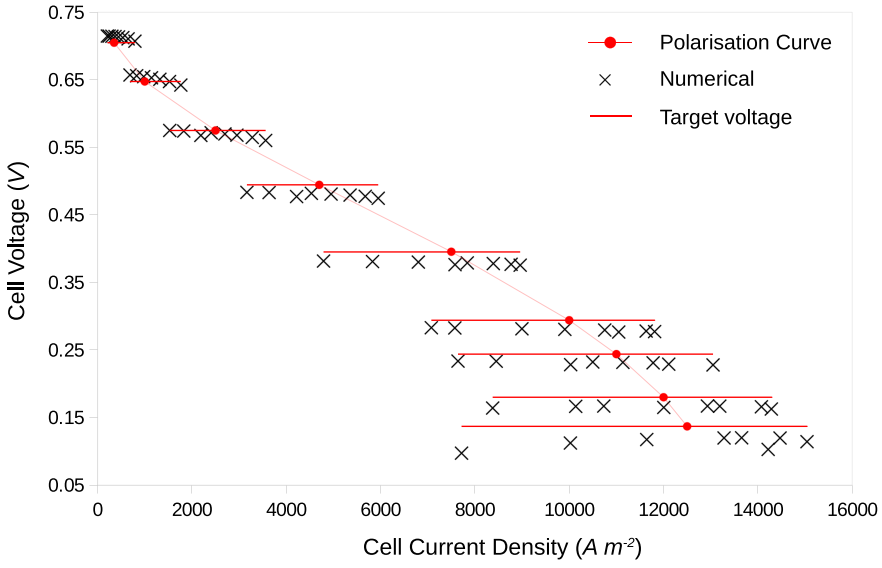

(a) Early in the process.

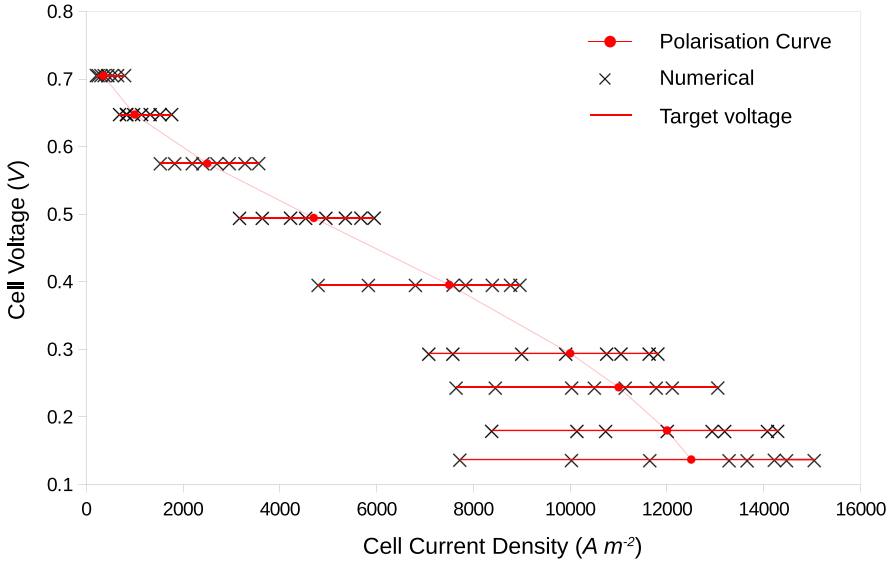

(b) At the end of the process

Fig. 5 – Representation of the calculated voltage $V_{[i,j]}$, and the experimental target values, $V_{exp[i]}$, for each of the locations analysed.

with the experimental ones. In this sense, since experimental data are subject to numerous measurement errors and deviations due to environmental and measurement conditions, increasing the amount of data beyond a certain point does not make much sense. Of course, it is necessary to carry out the simulations under the condition that the calculated intensity (the integral of the current density on the membrane) is equal to the intensity measured experimentally at each point of the polarisation curve.

Initial simulation

At the start, there is not any existing flow field solution to be used and only the experimental I_i, $i = 1, \ldots, z$ are available as input data. Taking a look at Diagram 9, a simple functioning approach has been derived. For this first iteration, I_i is considered uniformly distributed along the catalyst layers, so the density currents in the mentioned diagram j_a, j_c, are constant. An initial flow field can then be obtained, and from it the

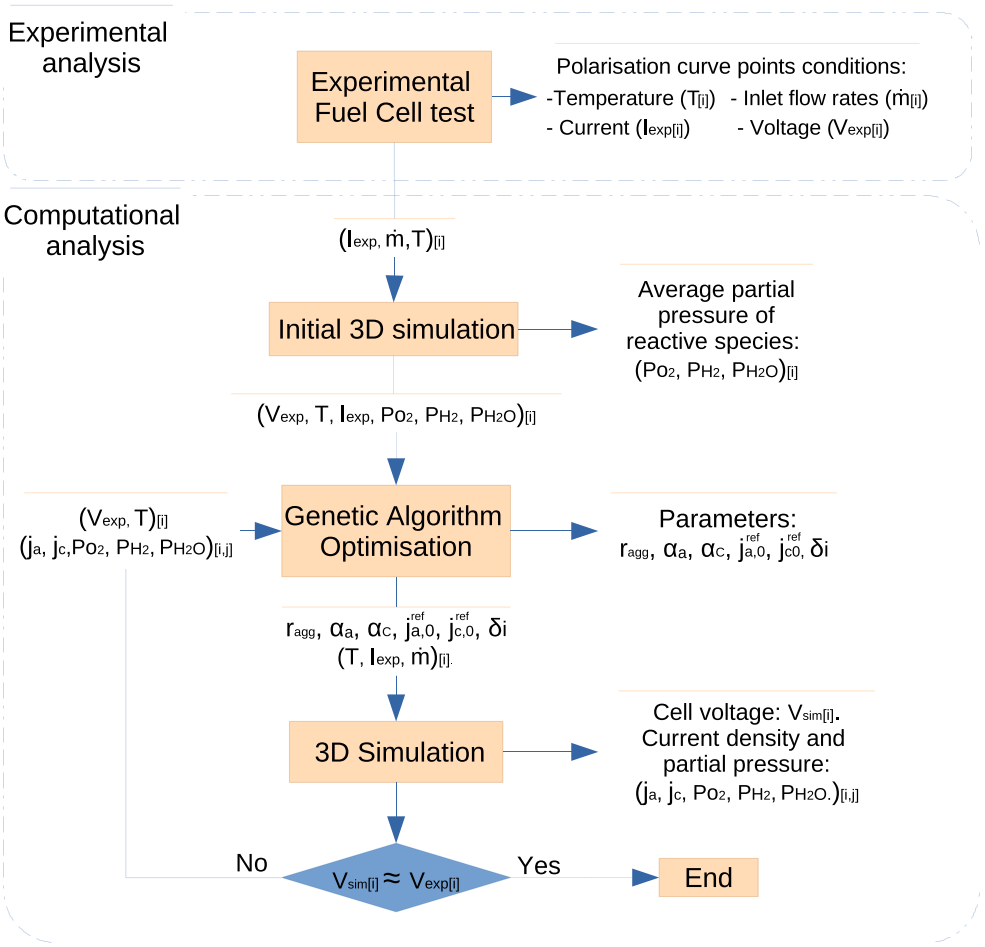

Fig. 6 – Diagram of the characterisation process through a combination of GA and CFD. Where i represents the points of the polarisation curve and j the number of locations selected at each point.

partial pressures (P_{O_2}, P_{H_2}, P_{H_2O}) at the catalyst layers. It has been observed that averaging these partial pressures provides a more robust starting point of iteration. With all this information, the genetic algorithm may start testing individuals in order to choose the optimal one. Notice that for this first iteration, since j_a, j_c, P_{O_2} are constant, the interval of possible values is reduced to a point, so $s = 1$. Once the optimal individual is obtained, the general iteration procedure shown in the previous subsection may begin. The whole algorithm is summarised in Fig. 6.

Two computational tools have been developed to implement this algorithm, both of which include the two electrochemical models described previously: a 3D simulation module for HTPEMFC in OpenFOAM and a C++ code for optimisation using genetic algorithms. It is recognised that even with the improvements shown in this section, the biggest CPU load still resides in the 3D simulations and the main feature of the optimisation step is robustness. For this purpose the readily available in-house genetic algorithm technique developed by the authors in Mustata et al. [22] is employed. The selection of the optimal individual in each iteration has been implemented by incorporating the electrochemical equations to this genetic algorithm.

Table 3 – Parameters to be characterised, search ranges and values obtained after one and two optimisations.

Parameter	Range	1° Iter.	2° Iter.
α_a	[0–1]	0.667 1	0.674 8
α_c	[0–1]	0.945 2	0.962 3
$j_{a,0}^{ref}$ (A/m^2)	[0–5000]	163.63	161.03
$j_{c,0}^{ref}$ (A/m^2)	[0–0.005]	1.455×10^{-5}	1.185×10^{-5}

Results and discussions

The method presented has been applied to two case studies, each one for each electrochemical model developed in Section HTPEMFC Model and relevant parameters.

Buttler-Volmer model

In the first case study, the data extracted from the experimental polarisation curve, published by Valiño et al. [16], have been used. The fuel cell analysed is a small device, 2 × 2 cm, powered by a mixture of hydrogen and water steam at the anode and a mixture of oxygen and water steam at the cathode. The

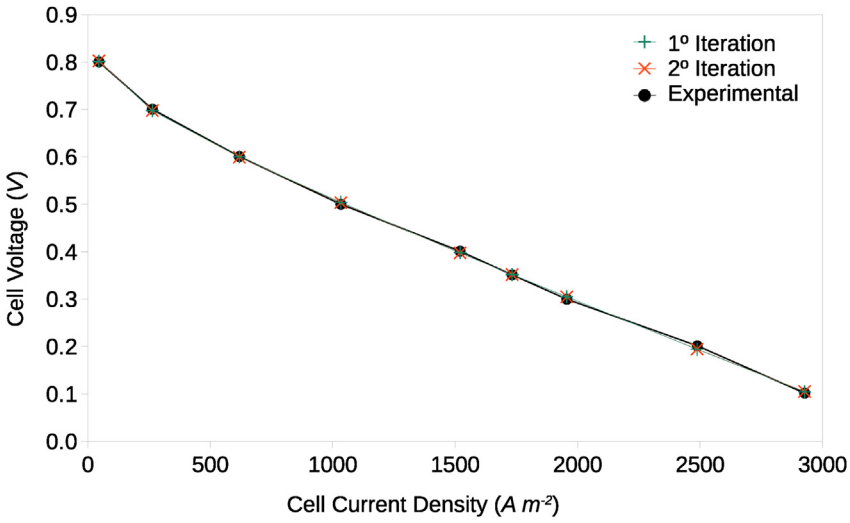

Fig. 7 – Simulated polarisation curves for each parameter optimisation vs. Experimental polarisation curve.

laboratory test was carried out at a constant temperature using cooling devices, which is necessary to ensure that the data obtained are consistent with an isothermal numerical model. The operating conditions of the different points of the curve and the physical and electrochemical parameters used for the simulations are shown in Table 2.

The range of parameter values to be optimised by the genetic algorithm is indicated in Table 3 and has been set according to their possible values within the described model. Bard et al. [17], report that the transfer coefficients, α_c and α_a, can range from zero to unity. According to Barbir [18], the exchange current density at 25 °C and 1 atmosphere for the reactions of hydrogen oxidation and oxygen reduction, with platinum catalytic, values are around 1×10^{-3} and 1×10^{-9} A cm^{-2}Pt respectively. In addition, the maximum electrolyte roughness value measured in fuel cells can reach 500 cm^2 of catalytic surface area per electrode geometric area, cm^2. In accordance with these references, the upper limit for the search for $j_{a,0}^{ref}$ and $j_{c,0}^{ref}$ has been set at 5000 and 0.005 A m^{-2} respectively.

By applying the process described above, and after performing two iterations through the characterisation loop, we obtain the sets of characterised parameters shown in Table 3, and the polarisation curves illustrated in Fig. 7. In both cases the curves obtained fit the experimental values, with a root mean square deviation value of 0.00374 V and 0.00371 V respectively. The fact that the curves converge after the first optimisation is due to the operating conditions of the experimental phase being such that they give rise to almost uniform distributions of the species along the catalyst layer and therefore the non-linearity of the electrochemical models is attenuated.

It is worth mentioning that the characterised parameters differ from those shown in Valiño et al. [16], because different models have been used to calculate both the overpotentials and the Nernst potential value.

Notice that the discrepancies between the simulated and experimental polarisation curves are due to a combination of the simplifications of the numerical model itself and the quality of the information extracted from the experimental phase.

Table 4 – Physical properties and operation conditions.

Parameter		Value
Inlet stoichiometric ratio		1.5
Inlet mass concentration	C_{H_2O}	0.218
(anode)	C_{H_2}	0.782
Inlet mass concentration	C_{H_2O}	0.02
(cathode)	C_{O_2}	0.23
	C_{N_2}	0.75
Temperature (K)	T	393
Reference pressure (atm)	P^{ref}	1
Reference temperature (K)	T^{ref}	353
Energy activation Anode ($J\ mol^{-1}$)	Ea	16 900
Energy activation Cathode ($J\ mol^{-1}$)	Ec	72 400
Porosity	ε	0.5
Anode pressure dependency coefficient	γ_a	0.5
Cathode pressure dependency coefficient	γ_c	1
Protonic conductivity (S m^{-1})	σ	2.9
Cathode catalyst layer thickness (m)	t_{CL}	1.25×10^{-5}
Volume fraction of ionomer	L_i	0.43
Pt loading ($kg\ m^{-2}$)	m_{pt}	0.004
Pt fraction	f	0.5

Agglomerated model

The second case study uses a numerical simulation to replace the data obtained in the experimental phase. This option has been considered because the operating conditions of the curve of the previous experiment do not reflect the concentration losses at high current densities. Furthermore, it is difficult to find polarisation curves for HTPEMFC in the literature that provide the necessary information in order to implement the process described in this article.

Besides, the numerically simulated experiment allows a better evaluation of the developed methodology as it eliminates the errors of the experimental measurements. In addition, it allows us to choose operating conditions that generate

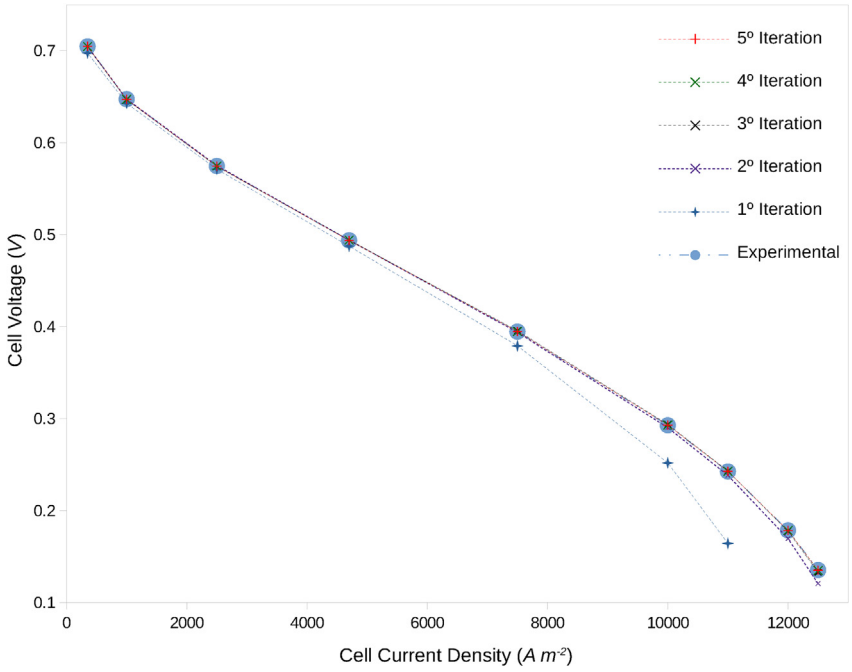

Fig. 8 – Simulated polarisation curves for each parameter optimisation vs. target polarisation curve. (Eight locations case).

Table 5 – Root mean square deviation of the polarisation curves obtained for each number of location selection and iteration. Units in V.

Locations	1°Iter.	2°Iter.	3°Iter.	4°Iter.	5°Iter.
Four	0.0368	0.00679	0.00124	0.00056	0.00041
Six	0.0368	0.01258	0.00141	0.00035	0.00021
Eight	0.0368	0.00632	0.00108	0.00027	0.00009

irregular current density distributions along the membrane and therefore to illustrate the potential of selecting locations from the internal regions in the optimisation process.

The same geometry has been used as in the previous case. For the range of values of the electrochemical properties of the agglomerate model, Sousa et al. [20] has been considered as a reference. Similar electrochemical models are used in that work and in the present one, avoiding the discrepancies found in the previous case. Both the electrochemical properties and the operating conditions chosen for the simulation are shown in Table 4.

Following the methodology described in Section Characterization process description, three characterisation experiments have been carried out on the same model, using a different number of locations (4, 6 and 8) in each point of the polarisation curve in order to see their influence on the process. In each of them, five iterations through the optimisation loop have been performed.

Fig. 8 shows the target and simulated polarisation curves using the optimised electrochemical parameters at each iteration for the case of eight locations. It can be observed that from the third iteration onward, the polarisation curves already show a reasonably good fit. The cases of 4 and 6 locations show similar behaviour and, visually, there are no major differences between the three cases. However, taking into account the value of the root mean square deviation shown in Table 5, it can be observed that in the following iterations the level of adequacy continues to improve. It can also be seen that, although there are no great differences, a greater number of locations allows to reach a better convergence.

Each simulation uses the optimised parameters under the pressure and current density conditions obtained from the previous simulation. The values used in the first simulation have been optimised on the basis of the data obtained from a simplification of the model as described in Section Initial simulation. Therefore, the result that it provides differs notably from the objective, since in this case of study, the

Table 6 – Parameters to be characterised, search ranges, values obtained in each iteration for the 8 locations characterisation case. Comparisons with experimental data.

Parameter	Range	1°Iter.	2°Iter.	3°Iter.	4°Iter.	5°Iter.	Exp.
α_a	[0.3–0.98]	0.651	0.397	0.666	0.567	0.802	0.5
α_c	[0.3–0.98]	0.803	0.749	0.731	0.742	0.736	0.74
$i_{a,0}^{ref}$ $(A\ m^{-2})$	[0–720 000]	240 418	456 734	631 923	706 203	717 221	80 559
$i_{c,0}^{ref}$ $(A\ m^{-3})$	[0–10 500]	1699	4100	5242	4554	4974	4708
δ_i (nm)	[5–100]	18.7	18.5	20.3	18.6	18.9	19.1
r_{agg} (nm)	[50–1000]	142	119	98	115	112	110

operating conditions cause the non-linearity of the equations to be manifested. In the subsequent ones, the data are obtained from a complete simulation and the optimisation is carried out using the different locations for each point of the polarisation curve.

In this case study, the values of the parameters to be characterised are known, since the information that replaces the experimental curve has been carried out by means of a numerical simulation. This allows the optimised parameters to be compared with the objectives and, in this way, to evaluate the identification capability of the developed methodology.

Table 6 shows the values of the parameters characterised in each iteration of the optimisation process for the case of eight locations, the target values used to obtain the experimental curve and the search ranges used. The characterisation of the parameters for the other two cases, with a smaller number of locations, show similar results although with a slightly lower performance with respect to the target values. The search limits for the parameters have been set according to their possible values in the electrochemical model used. As mentioned in section Buttler-Volmer model, the transfer coefficients can take values between 0 and 1.

According to the data provided by Sousa et al. [20], the reference current densities per unit catalytic area at 80 °C and 1 atm are 1.44×10^3 and 2.63×10^{-4} A $m^{-2}Pt$. To obtain the reference current densities as a function of geometrical area, these values are multiplied by the anode and cathode electrolyte roughness, 56 and 223.7 cm^2 of catalytic surface area per electrode geometric area, cm^2. It is also necessary to multiply $j_{c,0}^{ref}$, by the thickness of the catalyst layer to express its value as a function of the geometric volume and thus fit the equations of the implemented model. The upper limits for searching the reference current densities have been set considering the values provided by Sousa et al. [20] and a maximum roughness of 500 of catalytic surface area per electrode geometric area in both cases. There is a wide variety of values in the literature concerning the dimensions and composition of agglomerates. According to the Review of Agglomerate Model Parameters collected by Dobson et al. [14] and Li S. et al. [19], δ_i values can vary from 55 nm to 100 nm, while the agglomerate radius can range from 50 nm to 1000 nm.

Table 6 shows a better agreement of certain parameters compared to others. This is because their influence on the model is much greater. The properties of the agglomerate, δ_i and r_{agg} exhibit a better fit due to the fact that under the simulated operating conditions there is a strong influence of the concentration loss phenomenon. The values of the transfer coefficient and the reference exchange current density at the cathode also have a great influence on the model and it can be seen that both have a high fit to the target, and that this is enhanced at each iteration of the characterisation process. The anode parameters, on the other hand, not only show a poor fit in the last optimisation, but their values have erratic fluctuations in previous iterations, showing that the model sensitivity to these parameters is significantly lower. The results obtained are in line with those shown in the literature, since it is the cathode values that have the greatest influence and, therefore, those that the optimisation process best characterises.

Conclusions

The present work develops a methodology and corresponding numerical tools that allow for the characterisation of electrochemical parameters of HTPEMFCs that are difficult to measure experimentally. In contrast with previous works, full 3D models have been used. This enhances the accuracy in the representation of the device behaviour, a most needed property in parameter characterisation. The procedure involves the use of a genetic algorithm in order to search for the best electrochemical values iteratively. In each iteration, the fluid dynamics field is frozen and only electrochemical equations are solved by the genetic algorithm during the optimisation. The fluid dynamic fields are upgraded at the end of the iteration. This approach significantly reduces the computational cost, making the procedure feasible on a personal computer.

The methodology presented in this paper has been validated for two different electrochemical models. As future work, this technique can also be used to study the loss of efficiency of fuel cells by following the degradation of their parameter values at different points in their life cycle. This would help to derive improved degradation models. Thermal equations would need to be included in most of these studies. Other points of improvement are the analysis of sensitivity and collinearity between parameters, such as the one carried out by Goshtasbi et al. [23]. This kind of analysis would help with the selection of the parameters to be optimised, as well as the design of experimental conditions that would minimise possible collinearity issues among model parameters. Finally, for some cases, it could be interesting to explore the performance of other optimisation alternatives, besides the genetic algorithm used in this paper.

Declaration of competing interest

The authors declare that they have no known competing financial interests or personal relationships that could have appeared to influence the work reported in this paper.

Acknowledgements

The authors would like to acknowledge the financial support provided by the Spanish Ministry of Science and Innovation under the project DOVELAR (ref.: RTI2018-096 001-B-C31) and to the Aragon Government under the project LMP246_18. Support of the Regional Government of Aragon to the Fluid Mechanics for a Clean Energy Research Group (T01_20R) of the LIFTEC is also acknowledged.

REFERENCES

[1] Looney B. Statistical review of world energy. 69th ed. Bp; 2020.
[2] Quarton CJ, Samsatli S. Power-to-gas for injection into the gas grid: what can we learn from real-life projects, economic

assessments and systems modelling?. 2018. https://doi.org/10.1016/j.rser.2018.09.007.
[3] Ebrahimi S, Ghorbani B, Vijayaraghavan K. Optimization of catalyst distribution along PEMFC channel through a numerical two-phase model and genetic algorithm. Renew Energy 2017. https://doi.org/10.1016/j.renene.2017.06.067.
[4] Mo ZJ, Zhu XJ, Wei LY, Cao GY. Parameter optimization for a PEMFC model with a hybrid genetic algorithm. Int J Energy Res 2006. https://doi.org/10.1002/er.1170.
[5] Ali M, El-Hameed MA, Farahat MA. Effective parameters' identification for polymer electrolyte membrane fuel cell models using grey wolf optimizer. Renew Energy 2017. https://doi.org/10.1016/j.renene.2017.04.036.
[6] Ariza HE, Correcher A, Sánchez C, Pérez-Navarro Á, García E. Thermal and electrical parameter identification of a proton exchange membrane fuel cell using genetic algorithm. Energies 2018. https://doi.org/10.3390/en11082099.
[7] Zhu X, Wang N. Cuckoo search algorithm with onlooker bee search for modeling PEMFCs using T2FNN. Eng Appl Artif Intell 2019. https://doi.org/10.1016/j.engappai.2019.07.019.
[8] Brammya G, Praveena S, Ninu Preetha NS, Ramya R, Rajakumar BR, Binu D. Deer hunting optimization algorithm: a new nature-inspired meta-heuristic paradigm. Comput J 2019. https://doi.org/10.1093/comjnl/bxy133.
[9] Yuan Z, Wang W, Wang H, Yildizbasi A. Developed Coyote Optimization Algorithm and its application to optimal parameters estimation of PEMFC model. Energy Rep 2020. https://doi.org/10.1016/j.egyr.2020.04.032.
[10] Bao S, Ebadi A, Toughani M, Dalle J, Maseleno A, Baharuddin, Yıldızbası A. A new method for optimal parameters identification of a PEMFC using an improved version of Monarch Butterfly Optimization Algorithm. Int J Hydrogen Energy 2020. https://doi.org/10.1016/j.ijhydene.2020.04.256.
[11] Rizk-Allah RM, El-Fergany AA. Artificial ecosystem optimizer for parameters identification of proton exchange membrane fuel cells model. Int J Hydrogen Energy 2020. https://doi.org/10.1016/j.ijhydene.2020.06.256.
[12] Yang B, Zeng C, Wang L, Guo Y, Chen G, Guo Z, Chen Y, Li D, Cao P, Shu H, Yu T, Zhu J. Parameter identification of proton exchange membrane fuel cell via Levenberg-Marquardt backpropagation algorithm. Int J Hydrogen Energy 2021. https://doi.org/10.1016/j.ijhydene.2021.04.130.
[13] Ohenoja M, Leiviskä K. Observations on the parameter estimation problem of polymer electrolyte membrane fuel cell polarization curves. 2020. https://doi.org/10.1002/fuce.201900155.
[14] Dobson P, Lei C, Navessin T, Secanell M. Characterization of the PEM fuel cell catalyst layer microstructure by nonlinear least-squares parameter estimation. J Electrochem Soc 2012. https://doi.org/10.1149/2.041205jes.
[15] Goshtasbi A, Chen J, Waldecker JR, Hirano S, Ersal T. Effective parameterization of PEM fuel cell models—Part II: robust parameter subset selection, robust optimal experimental design, and multi-step parameter identification algorithm. J Electrochem Soc 2020. https://doi.org/10.1149/1945-7111/ab7092.
[16] Valiño L, Mustata R, Dueñas L. Consistent modeling of a single PEM fuel cell using Onsager's principle. Int J Hydrogen Energy 2013. https://doi.org/10.1016/j.ijhydene.2013.09.145.
[17] Bard AJ, Faulkner LR. Electrochemical methods: fundamentals and applications. New York: Wiley; 2001 [Russian Journal of Electrochemistry].
[18] Barbir F. Fuel cell basic chemistry and thermodynamics. In: PEM fuel cells; 2013. https://doi.org/10.1016/b978-0-12-387710-9.00002-3.
[19] Li S, Yuan J, Xie G, Sundén B. Effects of agglomerate model parameters on transport characterization and performance of PEM fuel cells. Int J Hydrogen Energy 2018. https://doi.org/10.1016/j.ijhydene.2018.03.106.
[20] Sousa T, Mamlouk M, Scott K. A non-isothermal model of a laboratory intermediate temperature fuel cell using PBI doped phosphoric acid membranes. Fuel Cell 2010. https://doi.org/10.1002/fuce.200900178.
[21] Klinedinst K, Bett JA, Macdonald J, Stonehart P. Oxygen solubility and diffusivity in hot concentrated H3PO4. J Electroanal Chem 1974. https://doi.org/10.1016/S0022-0728(74)80053-7.
[22] Mustata R, Harris SD, Elliott L, Ingham DB, Lesnic D. Retrieval of spacewise dependent hydraulic properties of anisotropic rocks from transient flow experiments. Transport Porous Media 2002. https://doi.org/10.1023/A:1015676111387.
[23] Goshtasbi A, Chen J, Waldecker JR, Hirano S, Ersal T. Effective parameterization of PEM fuel cell models—Part I: sensitivity analysis and parameter identifiability. J Electrochem Soc 2020. https://doi.org/10.1149/1945-7111/ab7091.